JVI Journals.ASM.org

Deletion of the ORF9p Acidic Cluster Impairs the Nuclear Egress of Varicella-Zoster Virus Capsids

Laura Riva,[a]* Marc Thiry,[b] Marielle Lebrun,[a] Laurent L'homme,[c] Jacques Piette,[a,c] Catherine Sadzot-Delvaux[a]

University of Liege, GIGA Infection Immunity and Inflammation, Laboratory of Virology and Immunology, Liege, Belgium[a]; University of Liege, GIGA Neurosciences, Laboratory of Cellular and Tissular Biology, Liege, Belgium[b]; University of Liege, GIGA Signal Transduction, Laboratory of Virology and Immunology, Liege, Belgium[c]

The protein encoded by ORF9 is essential for varicella-zoster virus (VZV) replication. Previous studies documented its presence in the *trans*-Golgi network and its involvement in secondary envelopment. In this work, we deleted the ORF9p acidic cluster, destroying its interaction with ORF47p, and this resulted in a nuclear accumulation of both proteins. This phenotype results in an accumulation of primary enveloped capsids in the perinuclear space, reflecting a capsid de-envelopment defect.

One of the crucial steps in herpesviruses infection is capsid exit from the nucleus. This process mainly follows the envelopment/de-envelopment model, strongly documented by transmission electron microscopy (TEM) observations (1). According to this model, nuclear capsids bud at the inner nuclear membrane (INM), thereby acquiring a primary envelope, which is then lost after fusion with the outer nuclear membrane (ONM), resulting in the release of naked capsids into the cytoplasm (1).

Viral glycoproteins seem to play a role during this de-envelopment fusion process (2). In the case of herpes simplex virus (HSV), it is known that gB and gH/gL, components of the viral entry machinery, are present at nuclear membranes and are likely responsible for this fusion (2, 3). Moreover, the fusogenic role of gB seems to be mediated by its pUS3-dependent phosphorylation (4). These hypotheses are supported by observations that HSV mutants lacking pUS3 or both gB and gH accumulate primary enveloped virions in the perinuclear space (3, 4). The components of the nuclear export complex (NEC), pUL31 and pUL34, have been described to mediate the primary envelopment (2). Phosphorylation of pUL31, another substrate of pUS3, also promotes the de-envelopment process (5).

Unfortunately, the mechanisms leading to varicella-zoster virus (VZV) nuclear egress are still poorly understood, and it is not clear whether the role of these proteins is conserved in VZV egress. In this work, we destroyed the interaction of the essential VZV tegument protein ORF9p (6) with the viral kinase ORF47p, homologous to HSV-1 VP22 and UL13, respectively, and this affected their localization and impaired VZV de-envelopment.

ORF9 is the most transcribed VZV gene during infection (7), and ORF9p has been observed to be present in the *trans*-Golgi network (TGN) (8), playing a role in secondary envelopment (9). Within its sequence is an acidic motif corresponding to residues 85 to 93: EDDFEDIDE (Fig. 1B). Acidic clusters are described as targeting signals to the TGN (10), and the HSV VP22 acidic cluster has been shown to have a role in both correct protein subcellular localization and virion incorporation (11). We thus deleted this acidic region to generate BAC-VZV-ORF9-ΔAC-V5 C-ter (Fig. 1A and B). Transfection of this bacterial artificial chromosome (BAC) into MeWo cells led to VZV-ORF9-ΔAC-V5 virus. Infection analysis revealed a significant defect in infectivity for this mutant, compared to that of the previously described VZV-ORF9-V5 (Fig. 1C) (9). Generation of the revertant VZV-ORF9-rev-V5, achieved by replacing the ORF9-ΔAC sequence with the wild-type one, rescued this defect (Fig. 1C).

In order to determine if this acidic region influences ORF9p localization, immunofluorescence analysis was performed on MeWo cells infected with VZV-ORF9-V5 (Fig. 2A to C), VZV-ORF9-ΔAC-V5 (Fig. 2D to F), or VZV-ORF9-rev-V5 (Fig. 2G to I). This experiment revealed the nuclear accumulation of ORF9p-ΔAC-V5 (Fig. 2D), compared to ORF9p-V5 or ORF9p-rev-V5, which appeared to be mainly cytoplasmic (Fig. 2A and G). ORF9p has been previously observed in the nucleus of infected cells by TEM analysis after immunogold labeling (8) and is characterized by the presence of two *in silico*-predicted nuclear localization signals (NLS) with the PSortII software (12); the first one has been confirmed to be active (13). Moreover, it contains an active nuclear export signal (NES) (13). This suggests that ORF9p can shuttle between the nucleus and cytoplasm, where its acidic region is thought to mediate its targeting to the TGN. Deletion of the ORF9p acidic region does not affect its isoelectric point or its *in silico*-predicted localization (PSortII prediction [12]), but it strongly modifies its subcellular localization.

This acidic cluster overlaps the consensus sequence SEDD (Fig. 1B), which we have previously described as being responsible for ORF47p-dependent phosphorylation (9). We thus decided to check the ORF9p-ΔAC Western blotting pattern in the context of infection. As shown in Fig. 2J to K (lanes 2 to 4), ORF9p-ΔAC migrated more quickly than ORF9p or ORF9p-rev in the gel, likely due to a reduced level of phosphorylation. In addition, coimmunoprecipitation experiments confirmed that the ORF9p-ORF47p

Received 5 November 2014 **Accepted** 26 November 2014

Accepted manuscript posted online 3 December 2014

Citation Riva L, Thiry M, Lebrun M, L'homme L, Piette J, Sadzot-Delvaux C. 2015. Deletion of the ORF9p acidic cluster impairs the nuclear egress of varicella-zoster virus capsids. J Virol 89:2436–2441. doi:10.1128/JVI.03215-14.

Editor: L. M. Hutt-Fletcher

Address correspondence to Catherine Sadzot-Delvaux, csadzot@ulg.ac.be.

* Permanent address: Laura Riva, Center for Infection and Immunity of Lille, Lille Pasteur Institute, University Lille North of France, Lille, France.

doi:10.1128/JVI.03215-14

A

Name	Sequence
BAC9DacR_GalK_F:	5'-ATAAAAATACGACCCCTCGCGTACATCAACCAAACGACTCCAGCGGA TCGCCTGTTGACAATTAATCATCGGCA-3'
BAC9DacR_GalK_R:	5'-TCTTCAACCAGTTCATGTCTCAAACGGGCCTCCCGAAAGGCGGCCAC TACTCAGCACTGTCCTGCTCCTT-3'
BAC9DacR_F:	5'-ATAAAAATACGACCCCTCGCGTACATCAACCAAACGACTCCAGCGGA TCGGTAGTGGCCGCCTTTCGGGAGGCCC-3'
BAC9DacR_R:	5'-TCTTCAACCAGTTCATGTCTCAAACGGGCCTCCCGAAAGGCGGCCAC TACCGATCCGCTGGAGTCGTTTGGTTGA-3'
dACrev_F:	5'-TAAAAATACGACCCCTCGCGTACATCAACCAAACGACTCCAGCGGAT CGGAAGATGACTTTGAAGACATCGATGAAGTA-3'
dACrev_R:	5'-CTTCAACCAGTTCATGTCTCAAACGGGCCTCCCGAAAGGCGGCCACT ACTTCATCGATGTCTTCAAAGTCATCTTCCGA-3'

B

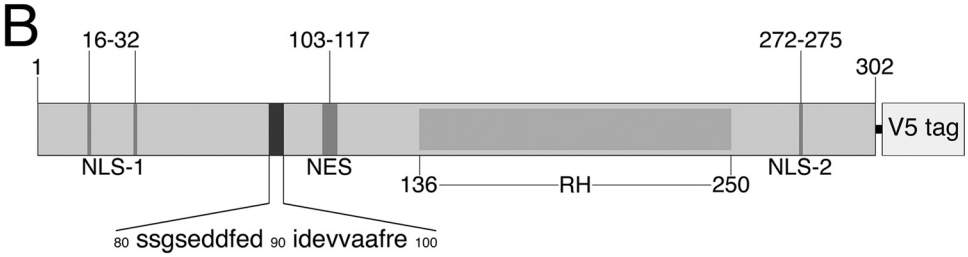

Acidic cluster:
AA 85-93: ssgsEDDFEDIDEvvaa

ORF47 binding site: $_{84}$SEDD$_{87}$

ΔAC: $_{80}$ssgs // vvaa$_{97}$

C

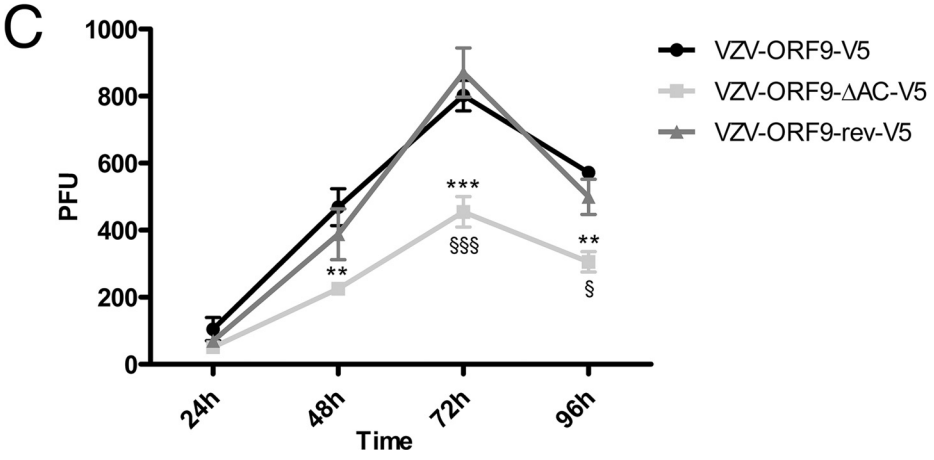

FIG 1 Deletion of the ORF9p acidic region impairs VZV infectivity. (A) Primer sequences used for the construction of recombinant viruses. (B) Schematic representation of the ORF9p mutant inserted in BAC-VZV, via a two-step BAC recombineering technique described by Warming et al. (21), generating the BAC-VZV-ORF9-ΔAC-V5 construct. ΔAC, deletion of the acidic cluster corresponding to amino acids (AA) 85 to 93 of ORF9p. (C) Analysis of VZV replication in MeWo cells. Uninfected cells were inoculated at day 0 with 200 infected cells for each infection (VZV-ORF9-V5, VZV-ORF9-ΔAC-V5, or VZV-ORF9-rev-V5), based on analysis by flow cytometry. Inoculated flasks were harvested daily for 4 days to perform serial dilutions. Infection quantification was performed after 2 days; we counted the fluorescent foci on melanoma cell monolayers. Each point represents the mean number of foci from three independent experiments. Error bars represent the standard errors of the means. RH, alphaherpesvirus conserved region of homology. Statistical significance is indicated by the following symbols (calculated by a two-way analysis of variance): **, $P < 0.01$, and ***, $P < 0.001$ (compared with VZV-ORF9-V5); §, $P < 0.05$, and §§§, $P < 0.001$ (compared with VZV-ORF9-rev-V5).

interaction observed for the wild type and the revertant was lost in cells infected with this ΔAC mutant (Fig. 2J and K, lanes 8).

Moreover, immunofluorescence analysis indicated a stronger nuclear accumulation of ORF47p in VZV-ORF9-ΔAC-V5-infected cells (Fig. 2E) than in VZV-ORF9-V5- or VZV-ORF9-rev-V5-infected cells (Fig. 2B and H). This observation suggests an involvement of ORF9p in exporting ORF47p from the nucleus to the cytoplasm or in its cytoplasmic retention. All experiments were performed as previously described (9).

In order to better understand the phenotype of this ΔAC mu-

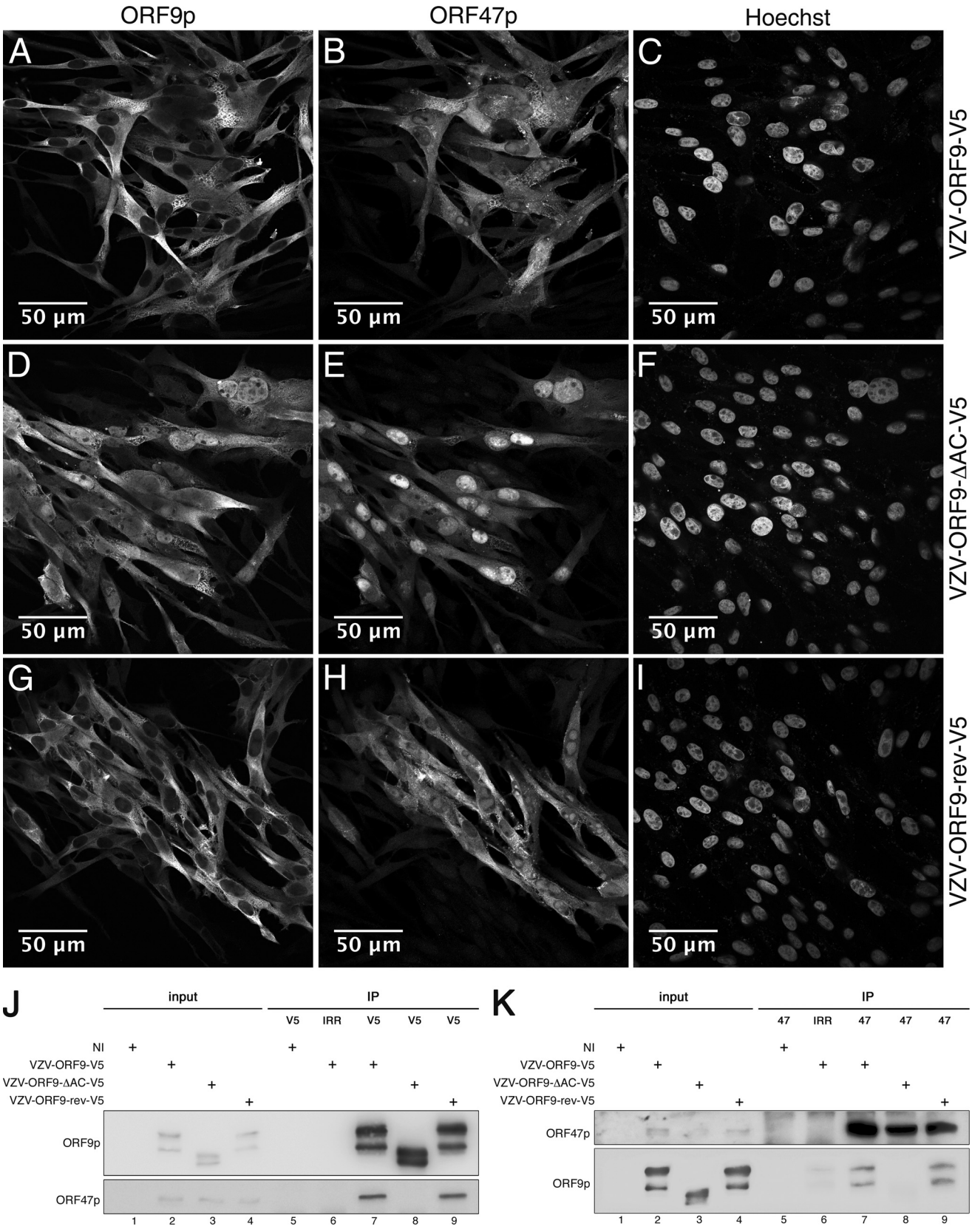

FIG 2 Deletion of the ORF9p acidic region leads to ORF9p and ORF47p nuclear accumulation. MeWo cells infected with VZV-ORF9-V5 (A to C), VZV-ORF9-ΔAC-V5 (D to F), or VZV-ORF9-rev-V5 (G to I) for 48 h were fixed using 4% paraformaldehyde and immunostained using the anti-V5 antibody (A, D, and G) or ORF47p antiserum (B, E, and H). Alexa 568 anti-rabbit and Alexa 633 anti-mouse were used as secondary antibodies. (C, F, and I) Nuclear labeling with Hoechst stain. Imaging was performed using a Zeiss 780 confocal microscope with a 63× oil objective. (J and K) Uninfected MeWo cells or MeWo cells infected for 24 h with VZV-ORF9-V5, VZV-ORF9-ΔAC-V5, or VZV-ORF9-rev-V5 were harvested in lysis buffer, and cell extracts were incubated with beads coated with anti-V5 antibody (J) or ORF47 antiserum (K). The immunoprecipitated proteins were resolved by SDS-PAGE and immunoblotted using antibody against the V5 tag and ORF47p antiserum. NI, noninfected cells; IRR, irrelevant antibody.

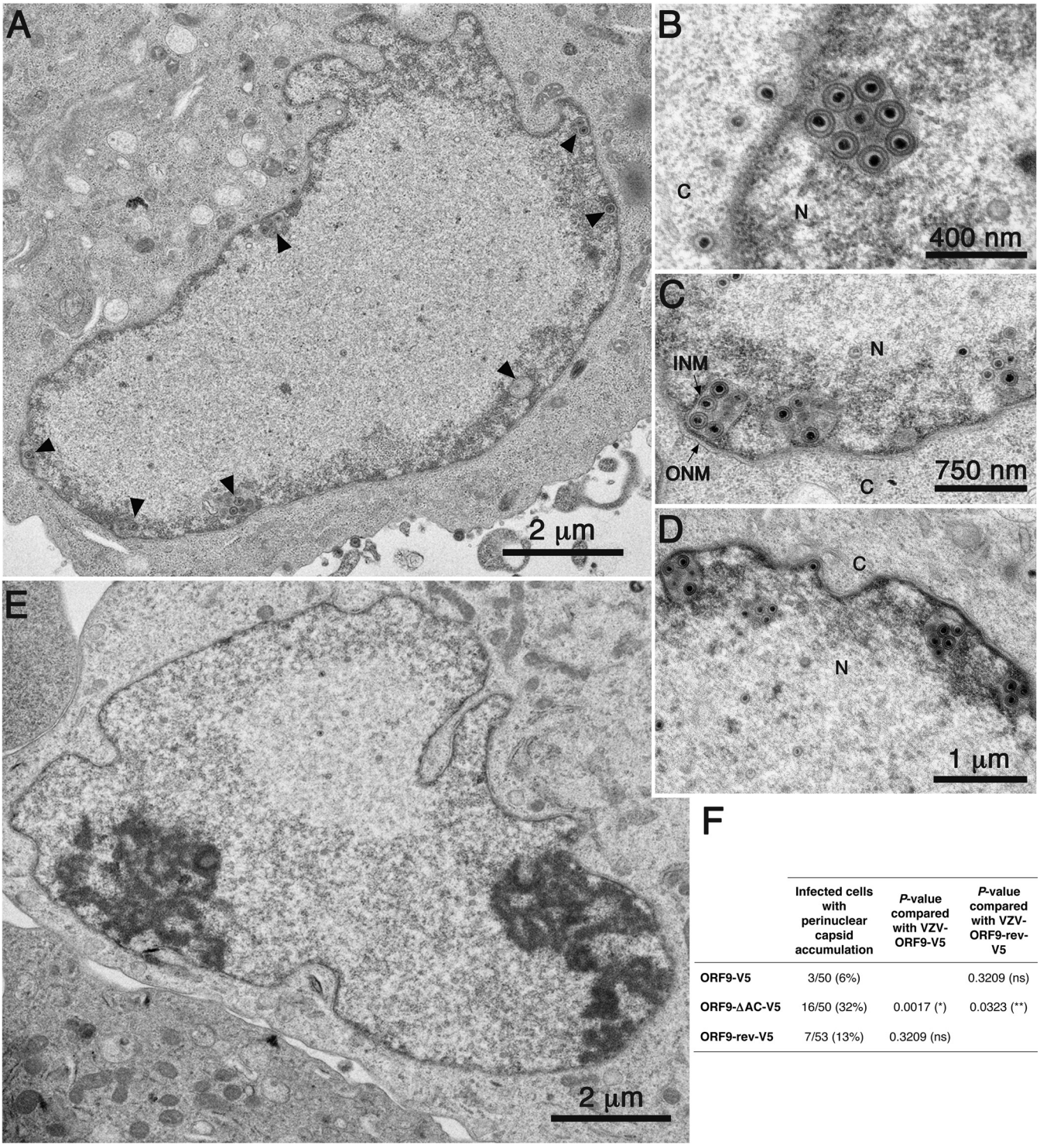

F

	Infected cells with perinuclear capsid accumulation	*P*-value compared with VZV-ORF9-V5	*P*-value compared with VZV-ORF9-rev-V5
ORF9-V5	3/50 (6%)		0.3209 (ns)
ORF9-ΔAC-V5	16/50 (32%)	0.0017 (*)	0.0323 (**)
ORF9-rev-V5	7/53 (13%)	0.3209 (ns)	

FIG 3 Deletion of the ORF9p acidic region causes an accumulation of primary enveloped capsids in the perinuclear space. MeWo cells were infected with VZV-ORF9-V5, VZV-ORF9-ΔAC-V5, or VZV-ORF9-rev-V5 for 48 h and then fixed and analyzed by TEM. (A to D) Nucleus of a VZV-ORF9-ΔAC-infected cell, representative of nuclear capsid accumulation (A), and higher magnifications of perinuclear spaces showing accumulations of primary enveloped VZV-ORF9-ΔAC capsids (B to D). (E) A nucleus representative of a VZV-ORF9-V5-infected cell. (F) Quantification of the observed phenotype. Cells infected with VZV-ORF9-V5, VZV-ORF9-ΔAC-V5, or VZV-ORF9-rev-V5 were analyzed for the presence or absence of perinuclear capsid accumulation, and the results are displayed in the table. Statistical significance was calculated by using Fisher's exact test and is indicated by one of the following symbols: *, $P < 0.05$; **, $P < 0.01$; ns, nonsignificant. N, nucleus; C, cytoplasm; INM, inner nuclear membrane; ONM, outer nuclear membrane. Arrowheads indicate perinuclear capsid accumulation.

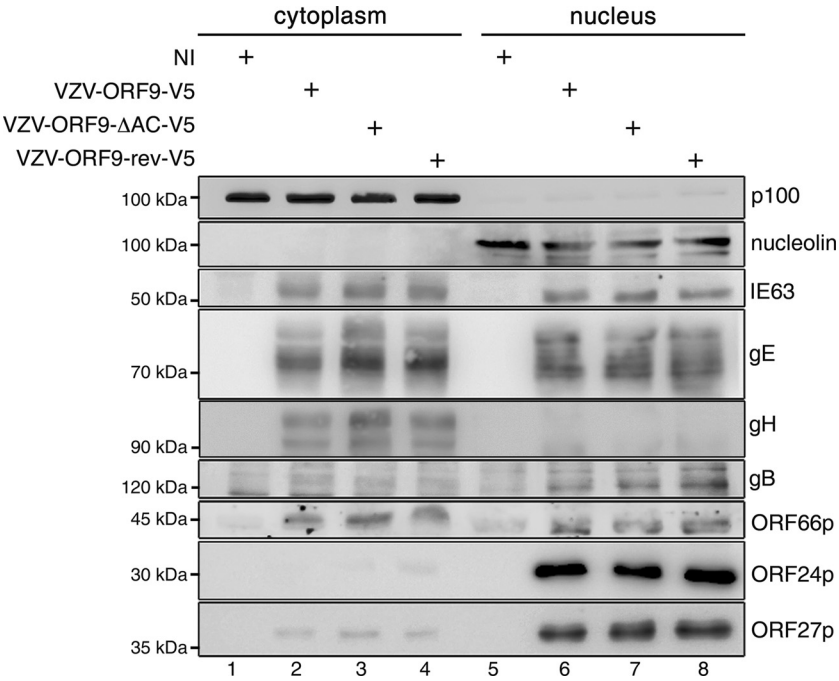

FIG 4 Proteins described as important players in the de-envelopment process are apparently not influenced by ORF9p mutation. (A) Noninfected MeWo cells or MeWo cells infected with VZV-ORF9-V5, VZV-ORF9-ΔAC-V5, or VZV-ORF9-rev-V5 for 24 h were harvested in cytoplasmic lysis buffer. After centrifugation, the pellet was washed and resuspended in nuclear lysis buffer. Cytoplasmic and nuclear proteins were resolved by SDS-PAGE and immunoblotted using antibodies against VZV IE63, gE, gH, ORF24p, and ORF27p and gB and ORF66p antisera. Cellular p100 and nucleolin C23 were used as the cytoplasmic and nuclear controls, respectively. NI, noninfected cells.

tant, VZV-ORF9-V5-, VZV-ORF9-ΔAC-V5-, and VZV-ORF9-rev-V5-infected MeWo cells were analyzed by TEM 48 h postinfection (Fig. 3). Surprisingly, the VZV-ORF9-ΔAC-V5-infected cells showed primary enveloped capsids that had accumulated in the perinuclear space (Fig. 3A to D versus E). Such perinuclear accumulation was observed in 32% of infected cells (up to 11 capsids/perinuclear structure), while it was observed in only 6% (maximum, 4 capsids) and 13% (maximum, 6 capsids) of wild-type- or revertant-infected cells, respectively (Fig. 3F). Altogether, these observations could explain the infection defect of VZV-ORF9-ΔAC-V5. ORF9p could be directly involved in capsid egress or have an indirect role, regulating ORF47p localization, which could itself regulate VZV de-envelopment. Another possibility is that neither ORF9p nor ORF47p are involved in capsid egress, but nuclear misaccumulation of one or both of these proteins could have an adverse effect on de-envelopment.

Nuclear and cytoplasmic extracts (14) from VZV-ORF9-V5-, VZV-ORF9-ΔAC-V5-, or VZV-ORF9-rev-V5-infected MeWo cells were further analyzed by Western blotting 24 h postinfection, in order to determine if the de-envelopment defect could be due to an altered expression level, stability, or localization pattern of gB, gH, ORF66p, ORF24p, or ORF27p, which are homologous to the HSV proteins involved in de-envelopment. The glycoprotein gE, described as an additional fusion protein during VZV entry (15), was also analyzed, while IE63 was chosen as an infection control. No apparent difference was observed for any of these proteins (Fig. 4), suggesting instead an independent role for ORF9p, which may act as a negative regulator of the fusion process. Observations of a pseudorabies mutant virus deleted for both gB and gH showed no defect in nuclear egress (16); indeed, this suggests that glycoprotein-mediated fusion is probably not the only mechanism involved in the de-envelopment process.

In summary, we showed that ORF9p is somehow involved in the ORF47p nuclear/cytoplasmic balance, and its acidic cluster was identified as an important determinant for ORF9p subcellular localization, ORF47p interaction, and VZV infectivity. We also found evidence that VZV nucleocapsid egress is impaired when the ORF9p acidic cluster is deleted.

ACKNOWLEDGMENTS

This work was supported by the Fonds pour la Recherche dans l'Industrie et l'Agriculture (Belgium) and by the Fonds National pour la Recherche Scientifique (Belgium). The study was cofunded by the University of Liege and the European Union via Marie Curie BeIPD DG Research-FP7-PEOPLE PCOFUND-GA-2012-600405 Fellowship.

We thank H. Zhu for BAC-VZV-pOka-WT (17), the Biology Research Branch at the NCI for the pGalK plasmid and SW102 bacterial strain, M. Sommer for gB and ORF66 antisera (18, 19), and S. Jonjic for anti-gH, ORF24, and ORF27 antibodies (20). We also thank P. Piscicelli for TEM preparations and the GIGA Imaging and GIGA Genotranscriptomics platforms for their technical support.

REFERENCES

1. **Mettenleiter TC, Muller F, Granzow H, Klupp BG.** 2013. The way out: what we know and do not know about herpesvirus nuclear egress. Cell Microbiol **15**:170–178. http://dx.doi.org/10.1111/cmi.12044.
2. **Johnson DC, Baines JD.** 2011. Herpesviruses remodel host membranes for virus egress. Nat Rev Microbiol **9**:382–394. http://dx.doi.org/10.1038/nrmicro2559.
3. **Farnsworth A, Wisner TW, Webb M, Roller R, Cohen G, Eisenberg R, Johnson DC.** 2007. Herpes simplex virus glycoproteins gB and gH function in fusion between the virion envelope and the outer nuclear mem-

brane. Proc Natl Acad Sci U S A **104:**10187–10192. http://dx.doi.org/10.1073/pnas.0703790104.

4. **Wisner TW, Wright CC, Kato A, Kawaguchi Y, Mou F, Baines JD, Roller RJ, Johnson DC.** 2009. Herpesvirus gB-induced fusion between the virion envelope and outer nuclear membrane during virus egress is regulated by the viral US3 kinase. J Virol **83:**3115–3126. http://dx.doi.org/10.1128/JVI.01462-08.
5. **Mou F, Wills E, Baines JD.** 2009. Phosphorylation of the U(L)31 protein of herpes simplex virus 1 by the U(S)3-encoded kinase regulates localization of the nuclear envelopment complex and egress of nucleocapsids. J Virol **83:**5181–5191. http://dx.doi.org/10.1128/JVI.00090-09.
6. **Tischer BK, Kaufer BB, Sommer M, Wussow F, Arvin AM, Osterrieder N.** 2007. A self-excisable infectious bacterial artificial chromosome clone of varicella-zoster virus allows analysis of the essential tegument protein encoded by ORF9. J Virol **81:**13200–13208. http://dx.doi.org/10.1128/JVI.01148-07.
7. **Cohrs RJ, Hurley MP, Gilden DH.** 2003. Array analysis of viral gene transcription during lytic infection of cells in tissue culture with varicella-zoster virus. J Virol **77:**11718–11732. http://dx.doi.org/10.1128/JVI.77.21.11718-11732.2003.
8. **Che X, Reichelt M, Sommer MH, Rajamani J, Zerboni L, Arvin AM.** 2008. Functions of the ORF9-to-ORF12 gene cluster in varicella-zoster virus replication and in the pathogenesis of skin infection. J Virol **82:**5825–5834. http://dx.doi.org/10.1128/JVI.00303-08.
9. **Riva L, Thiry M, Bontems S, Joris A, Piette J, Lebrun M, Sadzot-Delvaux C.** 2013. ORF9p phosphorylation by ORF47p is crucial for the formation and egress of varicella-zoster virus viral particles. J Virol **87:**2868–2881. http://dx.doi.org/10.1128/JVI.02757-12.
10. **Bonifacino JS, Traub LM.** 2003. Signals for sorting of transmembrane proteins to endosomes and lysosomes. Annu Rev Biochem **72:**395–447. http://dx.doi.org/10.1146/annurev.biochem.72.121801.161800.
11. **O'Regan KJ, Brignati MJ, Murphy MA, Bucks MA, Courtney RJ.** 2010. Virion incorporation of the herpes simplex virus type 1 tegument protein VP22 is facilitated by trans-Golgi network localization and is independent of interaction with glycoprotein E. Virology **405:**176–192. http://dx.doi.org/10.1016/j.virol.2010.06.007.
12. **Nakai K, Horton P.** 1999. PSORT: a program for detecting sorting signals in proteins and predicting their subcellular localization. Trends Biochem Sci **24:**34–36. http://dx.doi.org/10.1016/S0968-0004(98)01336-X.
13. **Cai M, Wang S, Xing J, Zheng C.** 2011. Characterization of the nuclear import and export signals, and subcellular transport mechanism of varicella-zoster virus ORF9. J Gen Virol **92:**621–626. http://dx.doi.org/10.1099/vir.0.027029-0.
14. **Bureau F, Delhalle S, Bonizzi G, Fievez L, Dogne S, Kirschvink N, Vanderplasschen A, Merville MP, Bours V, Lekeux P.** 2000. Mechanisms of persistent NF-kappa B activity in the bronchi of an animal model of asthma. J Immunol **165:**5822–5830. http://dx.doi.org/10.4049/jimmunol.165.10.5822.
15. **Maresova L, Pasieka TJ, Grose C.** 2001. Varicella-zoster virus gB and gE coexpression, but not gB or gE alone, leads to abundant fusion and syncytium formation equivalent to those from gH and gL coexpression. J Virol **75:**9483–9492. http://dx.doi.org/10.1128/JVI.75.19.9483-9492.2001.
16. **Klupp B, Altenschmidt J, Granzow H, Fuchs W, Mettenleiter TC.** 2008. Glycoproteins required for entry are not necessary for egress of pseudorabies virus. J Virol **82:**6299–6309. http://dx.doi.org/10.1128/JVI.00386-08.
17. **Zhang Z, Rowe J, Wang W, Sommer M, Arvin A, Moffat J, Zhu H.** 2007. Genetic analysis of varicella-zoster virus ORF0 to ORF4 by use of a novel luciferase bacterial artificial chromosome system. J Virol **81:**9024–9033. http://dx.doi.org/10.1128/JVI.02666-06.
18. **Oliver SL, Sommer M, Zerboni L, Rajamani J, Grose C, Arvin AM.** 2009. Mutagenesis of varicella-zoster virus glycoprotein B: putative fusion loop residues are essential for viral replication, and the furin cleavage motif contributes to pathogenesis in skin tissue in vivo. J Virol **83:**7495–7506. http://dx.doi.org/10.1128/JVI.00400-09.
19. **Schaap A, Fortin JF, Sommer M, Zerboni L, Stamatis S, Ku CC, Nolan GP, Arvin AM.** 2005. T-cell tropism and the role of ORF66 protein in pathogenesis of varicella-zoster virus infection. J Virol **79:**12921–12933. http://dx.doi.org/10.1128/JVI.79.20.12921-12933.2005.
20. **Lenac Rovis T, Bailer SM, Pothineni VR, Ouwendijk WJ, Simic H, Babic M, Miklic K, Malic S, Verweij MC, Baiker A, Gonzalez O, von Brunn A, Zimmer R, Fruh K, Verjans GM, Jonjic S, Haas J.** 2013. Comprehensive analysis of varicella-zoster virus proteins using a new monoclonal antibody collection. J Virol **87:**6943–6954. http://dx.doi.org/10.1128/JVI.00407-13.
21. **Warming S, Costantino N, Court DL, Jenkins NA, Copeland NG.** 2005. Simple and highly efficient BAC recombineering using galK selection. Nucleic Acids Res **33:**e36. http://dx.doi.org/10.1093/nar/gni035.